

# Privacy-preserving methods for smart-meter-based network simulations

Jordan Holweger<sup>a,\*</sup>, Lionel Bloch<sup>a</sup>, Christophe Ballif<sup>a</sup>, Nicolas Wyrsch<sup>a</sup>

<sup>a</sup>*Photovoltaic and thin film electronic laboratory, Ecole Polytechnique Fédérale de Lausanne, Neuchâtel, 2000, Switzerland*

---

## Abstract

Smart-meters are a key component of energy transition. The large amount of data collected in near real-time allows grid operators to observe and simulate network states. However, privacy-preserving rules forbid the use of such data for any applications other than network operation and billing. Smart-meter measurements must be anonymised to transmit these sensitive data to a third party to perform network simulation and analysis. This work proposes two methods for data anonymisation that enable the use of raw active power measurements for network simulation and analysis. The first is based on an allocation of an externally sourced load database. The second consists of grouping smart-meter data with similar electric characteristics, then performing a random permutation of the network load-bus assignment. A benchmark of these two methods highlights that both provide similar results in bus-voltage magnitude estimation concerning ground-truth voltage.

*Keywords:* smart-meter, privacy, anonymisation, load flow, network simulation

---

## 1. Introduction

The roll-out of smart-meters (SMs) in recent decades has enabled the collection of a large amount of data. Initially, meters were designed for billing purposes [1], but a wider range of applications is now available to utilities thanks to the valuable time-series collected. The processing of this data is often referred to as SM data analytics [2]. SMs are smart only because of their

---

\*Correspond author

*Email address:* jordan.holweger@epfl.ch (Jordan Holweger)

bi-directional communication capabilities [3] and their ability to perform automatic reading in comparison to conventional meters [1]. This enables the shedding of particular loads by the distribution system operator (DSO). The consumer can use the (near) real-time information of the consumption data to adapt and optimize its load and reduce its energy bill. Any additional functionality comes from the processing of the collected data, regardless of whether it is performed by the SM itself or remotely.

One well-known application is non-intrusive load monitoring (NILM) [4], which consists of disaggregating the whole-house electricity consumption into appliances/categories levels. This application is covered by extensive literature. Most applications of the NILM problem include a direct processing of the power measurement that is performed by the meter itself (or by a dedicated device) using the original high-sampling-frequency measurement [5]. Recent applications aim to disaggregate SM data in an offline phase as proposed by [6] and [7], i.e. by using lower-sampling-rate power measurements coming from SMs (typically a sampling rate of 15 min to 1 hour).

The second category of SM data analytics is to build typical customer profiles and extract their characteristics. This is often referred to as load profiling [8, 9]. The ultimate goal of such an identity map is to forecast flexibility as proposed by [10] or exploit typical load profile in a Monte-Carlo analysis [11]. Those typical profiles can be used in power-system planning studies. Alternatively, near real-time consumption information can be used to assess the network state. In an early phase of the SM roll-out, the communication infrastructure could not transmit data in real time but with a one-day delay [12]. In such a case, load forecasting was used to perform network state estimation. More recently, the time-asynchronization issue was addressed by [13] for similar purposes. The observability of the network depends on the availability [14] and location [15] of the SMs. While most SMs are located in low-voltage grids, the state of the medium voltage level can be inferred from these measurements reducing the need for adding further measurement devices at the low-voltage/medium-voltage transformer [16, 17]. The state estimation quality may also depend on the sampling frequency, as discussed in [18].

All the applications mentioned above do not account for the fact that SM data contains, by nature, sensitive information such as occupancy (which can potentially be predicted [19, 20, 21, 22, 23]). For this reason, data privacy has to be tackled from a regulatory perspective [24] and from a technical perspective [25]. There are evident conflicting interests between the data

owner (the households or the company being monitored) and the DSO or the energy retailer [26, 27]. The researchers of [27] proposed an approach to balance both interests. An early attempt at data anonymisation can be found in [28]. The researcher from [29] acknowledges that the final application is an important consideration to whether the DSO will be allowed to use the SM data. One approach to deal with the data privacy concern is to encrypt the SM measurements to restrict the ability of a third party to use the data only for specific purposes. The review of [30] proposes an extensive overview of various data-privacy-preserving approaches to transmitting SM data. A protocol based on multiparty computations is proposed in [31]. A differential privacy approach is used in [32], which allows customers to weigh the importance of privacy and pay for their chosen privacy level. Aggregation is often cited as the most computationally efficient approach to ensure privacy [33] but a drawback of aggregation is that aggregated data loses granularity and usefulness when performing the application mentioned above. Therefore, there is a need for a smart data-anonymisation approach that allows for the use of individual SM measurements in the context of power system studies.

Our work proposes and discusses two methods to use anonymous SM data for low-voltage network simulations. We define anonymity to mean the true locations of the SMs are unknown from the third party performing the simulations. In this work, we discuss network simulations as the final applications, but our proposed methods could be applied to further types of applications such as energy planning studies. Our approach relies on the assumption that the true consumption profile of customers can be replaced by any arbitrary load profile having similar characteristics and will provide similar results when performing load-flow simulations as if using the original one. The first method consists of allocating an anonymised load profile (i.e. SM data) in a network provided that the power exchange at the medium-voltage/low-voltage transformer is measured. The second method consists of anonymising the data by grouping and permuting SM measurements. The set of possible locations for a given SM group is the only information provided to the third party. By doing so, the user has no way to retrieve the original SM locations. This paper proposes two solutions for the DSO to exploit their metering data while ensuring the anonymity of their customers. Both approaches do not rely on advanced cryptography methods, requiring data processing at the meter level and on the third party's side. Both allow the final users to use raw SM data for their final applications. It allows building realistic load cases for network simulations or possibly other applications like

energy planning purposes.

This paper is structured as follows. Two approaches for SM anonymisation are proposed in section 2. The first is an allocation method (section 2.1) while the second is an anonymisation by grouping and permuting method (section 2.2). We compare both approaches using a dedicated benchmark presented in section 3. Section 4 presents key results and compares the performance, while section 5 discusses advantages and drawbacks. Finally, section 6 draws some conclusions.

## 2. Proposed anonymisation approaches

### 2.1. Smart-meter allocation

The basic idea of load profile allocation is to choose, from a sufficiently large dataset of load profiles, the most-appropriate ones according to some knowledge of the network and consumers' characteristics. The first stage consists in selecting these load profiles according to their annual consumption magnitude and category (residential, commercial, etc.). The loads are allocated to network locations according to prior knowledge of the consumers' annual consumption. Each load is scaled to ensure that the total network consumption is matched. A second stage is to deform the allocated load profiles so that the resulting load at the transformer is close enough to the measured transformer load, still keeping the annual energy consumption close to the original one. Thus, the developed methods consist in a two-stage optimization. In the first phase, a load profile is allocated to each meter. All profiles are tuned in the second phase to match potential additional network measurements. In particular, the sum of all the profiles should be as close as possible to the profile at the transformer (which should be known).

#### 2.1.1. First-stage optimisation

The overall idea of the first-stage optimization problem is to consider the grid as a graph, formed by a set of nodes  $N$ , among which the set  $N_L \subset N$  of nodes has unknown load profiles. The set  $N_K \subset N$  contains measured load profiles. The root node (or transformer) is denoted as  $N_P \subset N$ . The reference dataset of load profiles is considered as virtual nodes  $J$ . Any load profile is assumed to be measured on the same time span  $T$ . Finally, for each node  $n \in N_L$  and  $j \in J$  we define a load category  $h_n \in H$ . The sets' definitions are given in table 1. The problem can be defined as connecting each node in  $N_L$  to a single node in  $J$  of the same load category (as pictured

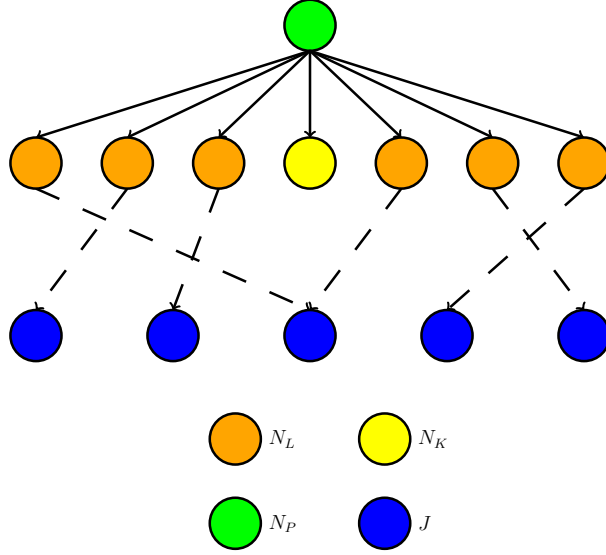


Figure 1: Illustration of the first-stage allocation

in fig. 1). The difference between the allocated annual energy consumption of the reference load profile,  $E_n^{\text{var}}$ , and the one from the meter (assumed to be known for every node),  $E_j^{\text{ref}}$ , should be smaller than a given tolerance  $\epsilon_E$ . In other words, the decision variable  $\beta_{n,j}$ , if greater than 0, allocates and scales the load profile  $j$  to the node  $n$  to have the allocated annual energy  $E_n^{\text{var}}$  close to the tolerance  $\epsilon_E$  of the measured annual consumption of the node  $E_n^{\text{ref}}$ . The optimization's objective is to have the minimum scaling of the available load, i.e.  $\beta_{n,j} \approx 1 \forall j \in J$ . As pictured in fig. 1, a single available load profile may be allocated to more than one node in  $N_L$ . A parameter of the optimization problem  $k^h$  restricts the number of allocations for each load category. The size of  $N_L$  may be much larger than the size of  $J$ . Thus, each load can be allocated more than once in the network.

Table 1: Network topology and sets

Set	Subset of	Description
$N$	-	network nodes
$H$	-	load category
$N_P$	$N$	transformer node with measured load profiles
$N_L$	$N$	nodes with unknown load profiles
$N_L^{h \in H}$	$N_L$	nodes subset per load category
$N_K$	$N$	nodes with known load profiles
$J$	-	virtual nodes representing available load profiles from the dataset
$J^{h \in H}$	$J$	available load profiles subset per load category
$T$	-	time

The problem can be mathematically described as follows. A reference load's annual energy consumption  $E_j^{\text{ref}}$  is allocated to a node  $n$  if the Boolean variable  $\alpha_{n,j} = 1$  (1a). It can be optionally scaled by a factor  $\beta_{n,j} > 0$  (1b). The scaling factor is 0 when  $\alpha$  is 0 (1c). Only one reference load can be allocated to each node (1d). Each reference load can be allocated up to  $k^h$  times (1e). The parameters  $k^h$  are defined for each load category  $h \in H$  and aim to ensure a certain variety in the choice of the allocated load. An appropriate choice for these parameters is  $k^h = \left\lceil \frac{N_L^h}{J^h} \right\rceil \forall h \in H$ . Assuming the annual energy demand for each node is known (either directly or by estimation), the scaled load profile should have an annual energy demand

close to the reference one up to a given tolerance  $\epsilon_E$  (1f).

$$E_n^{\text{org}} = \sum_{j \in J^h} \alpha_{n,j} E_j^{\text{ref}} \quad \forall n \in N_L^h, h \in H \quad (1a)$$

$$E_n^{\text{var}} = \sum_{j \in J^h} \beta_{n,j} E_j^{\text{ref}} \quad \forall n \in N_L^h, h \in H \quad (1b)$$

$$\alpha_{n,j} = \begin{cases} 0, & \text{if } \beta_{n,j} = 0 \\ 1, & \text{otherwise} \end{cases} \quad \forall n \in N_L^h, j \in J^h, h \in H \quad (1c)$$

$$\sum_{j \in J^h} \alpha_{n,j} = 1 \quad \forall n \in N_L^h, h \in H \quad (1d)$$

$$\sum_{n \in N_L^h} \alpha_{n,j} \leq k^h \quad \forall j \in J^h, h \in H \quad (1e)$$

$$\epsilon_E^2 \geq 1 - \frac{2 \cdot E_n^{\text{var}}}{E_n^{\text{ref}}} + \frac{(E_n^{\text{var}})^2}{(E_n^{\text{ref}})^2} \quad \forall n \in N_L \quad (1f)$$

The optimal allocation problem aims to make the value of  $\beta_{n,j}$  as close as possible to 1. This is translated into a quadratic objective function (2) which aims to minimize the difference between the allocated energy  $E^{\text{org}}$ , and the scaled energy,  $E^{\text{var}}$ . Besides, having the constraints applied to subset  $N_L^h$  and performing a sum over  $J^h$  ensure that the load category matches without introducing any additional binary variable. All parameters and decision variables are described in table 2.

$$\begin{aligned} & \min && \sum_{n \in N_L} (E_n^{\text{org}})^2 - 2 \cdot E_n^{\text{org}} \cdot E_n^{\text{var}} + (E_n^{\text{var}})^2 \\ & \text{for} && \beta_{n,j} \\ & \text{subject to:} && (1a) \text{ to } (1f) \end{aligned} \quad (2)$$

### 2.1.2. Second-stage optimization

The second stage reuses the allocated load profile,  $P^{\text{org}}$ (3a). It tunes the allocated load profiles using a time-varying variable  $\gamma_{n,t}$  (3b) to match the resulting power profile at the transformer node,  $P_{NP,t}^{\text{var}}$  (3c) with the measured power profile  $P_{NP,t}^{\text{ref}}$ , i.e. having the relative difference between both under a given tolerance  $\epsilon_P$  (3d). Additionally, the constraints on the annual energy consumption (3e) still apply (3f). The optimization problem's goal is to

deform the load profiles as little as possible, hence having  $\gamma_{n,t} \approx 1 \forall n \in N^L, t \in T$  (4).

$$P_{n,t}^{\text{org}} = \sum_{j \in J} \alpha_{n,j} P_{j,t}^{\text{ref}} \quad \forall n \in N_L, t \in T \quad (3a)$$

$$P_{n,t}^{\text{var}} = \gamma_{n,t} P_{n,t}^{\text{org}} \quad \forall n \in N_L, t \in T \quad (3b)$$

$$P_{N_P,t}^{\text{var}} = \sum_{n \in N_L} P_{n,t}^{\text{var}} + \sum_{n \in N_K} P_{n,t}^{\text{ref}} \quad \forall t \in T \quad (3c)$$

$$\epsilon_P^2 \geq 1 - \frac{2 \cdot P_{N_P,t}^{\text{var}}}{P_{N_P,t}^{\text{ref}}} + \frac{(P_{N_P,t}^{\text{var}})^2}{(P_{N_P,t}^{\text{ref}})^2} \quad \forall t \in T \quad (3d)$$

$$E_n^{\text{var}} = \sum_{t \in T} P_{n,t}^{\text{var}} \cdot T S_t \quad \forall n \in N_L \quad (3e)$$

$$\epsilon_E^2 \geq 1 - \frac{2 \cdot E_n^{\text{var}}}{E_n^{\text{ref}}} + \frac{(E_n^{\text{var}})^2}{(E_n^{\text{ref}})^2} \quad \forall n \in N_L \quad (3f)$$

$$\begin{aligned} & \min && \sum_{n \in N_L} \sum_{t \in T} (P_{n,t}^{\text{org}})^2 - 2 \cdot P_{n,t}^{\text{org}} P_{n,t}^{\text{var}} + (P_{n,t}^{\text{var}})^2 \\ & \text{for} && \gamma_{n,t} \\ & \text{subject to:} && (3a) \text{ to } (3f) \end{aligned} \quad (4)$$

Table 2: Parameters and variables. Column **S** indicates first-stage or second-stage optimization variables.

	<b>S</b>	<b>Set</b>	<b>Dimension</b>	<b>Unit</b>	<b>Description</b>	
PARAMETERS		$\mathbb{R}_+$	$(N_P \cup N_K) \times T$	W	measured load	
	$P_{n,t}^{\text{ref}}$	$\mathbb{R}_+$	$(N_P \cup N_K) \times T$	W	measured load	
	$E_n^{\text{ref}}$	$\mathbb{R}_+$	$N_L \cup N_K$	J	measured annual consumption	
	$h_n$	$H$	$N_L \cup J$	-	load category	
	$k^h$	$\mathbb{N}_+$	$H$	-	maximum allocation per category	
	$\epsilon_E$	$\mathbb{R}_+$		-	relative tolerance on energy	
	$\epsilon_P$	$\mathbb{R}_+$		-	relative tolerance on power	
$TS_t$	$\mathbb{R}_+$	$T$		s	timesteps	
VARIABLES		1	$\mathbb{R}_+$	$N_L$	J	original annual consumption
	$E_n^{\text{org}}$	1	$\mathbb{R}_+$	$N_L$	J	original annual consumption
	$E_n^{\text{var}}$	1,2	$\mathbb{R}_+$	$N_L$	J	scaled annual consumption
	$\beta_{n,j}$	1	$\mathbb{R}_+$	$N_L \times J$	-	annual scale
	$\alpha_{n,j}$	1	$[0, 1]$	$N_L \times J$	-	allocation variable
	$\gamma_{n,t}$	2	$\mathbb{R}_+$	$N_L \times T$	-	timestep scale
	$P_{n,t}^{\text{org}}$	2	$\mathbb{R}_+$	$(N_L \cup N_P) \times T$	W	originally allocated load profiles
	$P_{n,t}^{\text{var}}$	2	$\mathbb{R}_+$	$(N_L \cup N_P) \times T$	W	allocated load profiles

## 2.2. Smart-meter anonymisation

In this section, we propose a SM anonymisation method for network simulations (SMANET). The approach considers that the link between the SM ID ( $i$ ) and its network location ( $b$ ) is known from the DSO metering service. Still, it cannot be communicated to the planners or any other third party for analysis without the data owner’s explicit and informed consent. However, the raw SM measurements and network topology are available for the DSO network planning service. The basic idea of this method is to group SM measurements according to some characteristic features and provide, for each group, the network location list corresponding to the group. In the graphical example of fig. 2, the meter IDs 1, 2, and 3 are assigned to group A (there can be as many groups as necessary). They are located in network locations a, b, and c, respectively. From the network planner’s perspective, the only information accessible is that  $i = 1, 2, \text{ and } 3$  are in the same group as  $b = a, b, \text{ and } c$ . The network planner can arbitrarily choose to allocate the SM measurements 1 to the location a, b, or c, etc. The underlying assumption is that the SM measurements 1, 2, and 3 are electrically similar because they are in the same group. Hence inverting  $i = 1$  and 2 at  $b = a$  should have a

minor impact on any further analysis performed by the network planner.

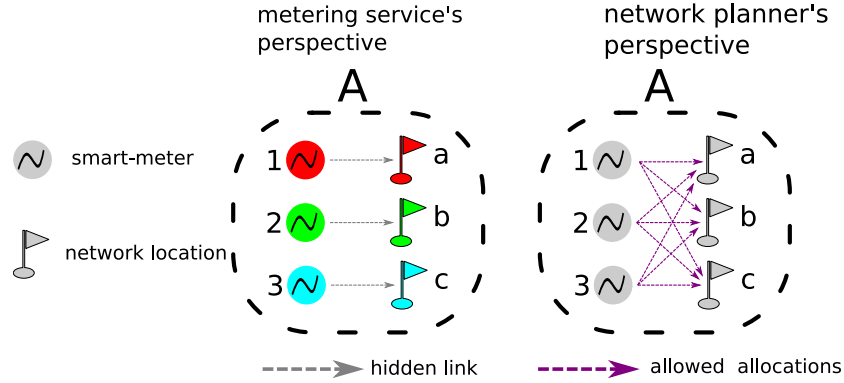


Figure 2: Graphical description of the SMANET method

The workflow for setting up an anonymous allocation of SM data into a designated network follows. The network planner receives the SM measurements  $P_{i,t}$ . The first task is to extract  $K \geq 1$  relevant features  $X_{i,k}$   $k = 1 \dots K$  for each measured load. The second task is to group the SMs according to their features. The grouping, more commonly known as clustering, has one additional constraint compared with standard clustering methods. The number of clusters is not known in advance, and the population size inside a cluster is pre-determined. Such a task is referred to as partitioning in the literature[34]. The population in each cluster should be more or less equal (balanced partitioning). At this stage, the metering service takes over and provides the list of buses for each meter group. Finally, the network planner randomly takes one permutation of the bus list to allocate each meter to a bus. This process is graphically pictured in fig. 3.

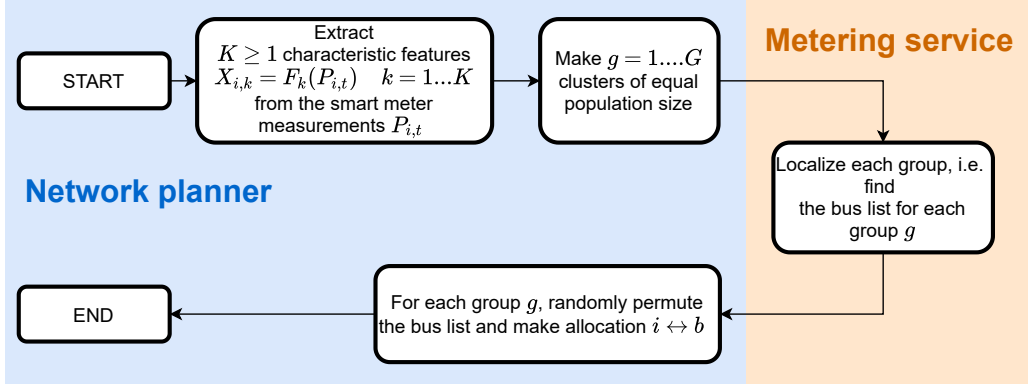


Figure 3: Workflow of the SMANET method

The critical step in this process is to form groups of an equal number of elements. This might be tackled from a clustering perspective (considering that the number of elements in each cluster  $m$  is predefined), such as in [35]. In the later derivation of the  $k$ -mean algorithm,  $m$  is quite large. For  $m = 2$ , mathematicians consider the stable roommates' problem [36]. The extension to triple roommates [37] or multi-dimensional roommates [38] is still an open research topic. In the following, we investigate partitioning techniques and propose a suitable algorithm to perform the partitioning of the SM measurements into groups of equal size.

### 2.2.1. Integer programming formulation of the partitioning problem

A generic formulation of the partitioning problem can be formulated using integer programming (IP)[39]. For a given dataset  $\mathbb{D}$  of  $N$  records and the similarity matrix  $D[N \times N]$ .  $D_{u,v} \in [0, \infty)$  is a measure of the similarity between records  $u$  and  $v$ . We assume that this similarity measure respects the identity of indiscernibles ( $D_{u,u} = 0$ ), is symmetric ( $D_{u,v} = D_{v,u}$ ) and respects the triangle inequality ( $D_{u,v} + D_{v,w} \geq D_{u,w}$ ). Typically such similarity metrics can be the Euclidian distance. Let  $x_u$  be a vector of  $K$  characteristic features. The similarity between two records can be calculated as  $D_{u,v} = \sqrt{\sum_{k=1}^K (x_{v,k} - x_{u,k})^2}$ . In the following, we will consider such a similarity measure but any other similarity measure respecting the space metric properties is suitable.

The balanced partitioning problem consists in splitting the dataset into  $N_C$  clusters in which the number of records per cluster is equal for all clusters.

One can deduce the prior relationship between the number of records per cluster and the number of clusters as

$$m \leq \frac{N}{N_C} < m + 1 \Rightarrow m = \left\lfloor \frac{N}{N_C} \right\rfloor$$

where  $\lfloor \cdot \rfloor$  is the floor function.

Let us now see the dataset as a graph  $\mathbb{G}$  where  $\mathbb{S}$  is the set of edges that connect pairs of records  $(u, v)$ . To keep the full generality, let's assume that the graph is coarse, i.e. some pairs  $(u, v)$  are not connected  $((u, v), (v, u) \notin \mathbb{S}$ . The edge weights are given by the similarity matrix  $D$ . The partitioning problem can be seen as connecting the records or nodes of  $\mathbb{G}$  to form an independent subgraph of  $\mathbb{G}$  containing between  $m$  and  $m + 1$  records. The selection of an edge between two records is represented by variable  $\delta_{u,v}$ :

$$\delta_{u,v} = \begin{cases} 1 & \text{if record } u \text{ is in the same cluster as } v \\ 0 & \text{otherwise} \end{cases} \quad (5)$$

The variable  $g_{c,u}$  keeps track of the belonging of record  $u$  to cluster  $c$  as

$$g_{c,u} = \begin{cases} 1 & \text{if record } u \text{ belongs to cluster } c \\ 0 & \text{otherwise} \end{cases} \quad (6)$$

Using these definitions, we can formulate the balanced partitioning problem as minimizing the sum of the selected edges' weights (8), subject to the following constraints: A pair of unconnected nodes cannot be in the same cluster (7a), each node must belong to exactly one cluster (7b), the number of elements per cluster is constrained (7c), and nodes  $u \in c$  and  $v \in c$  imply  $\delta_{u,v} = 1$  (7d). Conversely,  $u \in c$  and  $v \notin c$  imply  $\delta_{u,v} = 0$  (7e).

$$g_{c,u} + g_{c,v} \leq 1 \quad \forall (u, v) \notin \mathbb{S} \quad (7a)$$

$$\sum_{c=1}^{N_C} g_{c,u} = 1 \quad \forall u = [1 \dots N] \quad (7b)$$

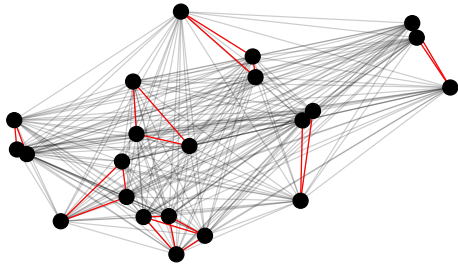
$$m \leq \sum_{u=1}^{N_C} g_{c,u} \leq m + 1 \quad \forall c = [1 \dots N_C] \quad (7c)$$

$$g_{c,u} + g_{c,v} - x_{u,v} \leq 1 \quad \forall (u, v) \in \mathbb{S} \quad (7d)$$

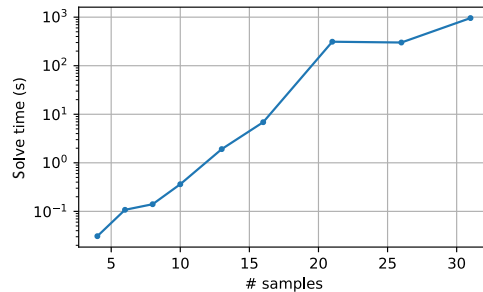
$$g_{c,u} + (1 - g_{c,v}) - (1 - x_{u,v}) \leq 1 \quad \forall (u, v) \in \mathbb{S} \quad (7e)$$

$$\begin{aligned}
& \min && \sum_{(u,v) \in \mathbb{S}} \delta_{u,v} \cdot D_{u,v} \\
& \text{for} && \delta_{u,v} \\
& \text{subject to:} && (7a) \text{ to } (7e)
\end{aligned} \tag{8}$$

Figure 4a illustrates the results of partitioning a fully connected graph of 22 nodes into seven clusters of three records. The partitioning into three records using this formulation is replicated for graphs with sizes ranging from 4 to 31 elements. For each problem, the time for solving is recorded and pictured in fig. 4b. This illustrates the issue with such a formulation. The computation time increases exponentially with the graph size. One can estimate that solving problems containing about 100 records would be in the range of  $10^8$  years. There is hence a need for a faster partitioning method.



(a) Illustration of graph partitioning: the red edges form the final five clusters



(b) Solving time

Figure 4: Graph partitioning with integer programming

### 2.2.2. Spectral graph partitioning

In modern computational science, graph partitioning is used mainly for balancing loads and minimizing scientific computation time [34] (for instance, to solve a sizeable computational fluid dynamic problem in parallel, the discretised space domain is split into smaller pieces to be individually solved on several cores). Another application concerns route planning [34].

Spectral graph partitioning is precisely described in [34] as the connection between cuts in a graph and its second smallest eigenvalue. To understand this relation, it is necessary to recall a few properties of a graph. Let  $G$  be a graph of  $n$  nodes and  $(i, j) \in S$ , its set of edges. Three matrices are

associated with such a graph. First, the adjacency matrix  $A$  of a weighted graph is defined as

$$A_{i,j} = \begin{cases} 0 & \text{if } i = j \\ w_{i,j} & \text{otherwise} \end{cases}$$

Assuming the edge weight  $w_{i,j}$  represents some sort of distance between two nodes, the adjacency matrix refers to the similarity matrix presented above. Second, the degree matrix is a diagonal matrix, where each element on its diagonal is the number of edges connecting this particular node:

$$D_{i,j} = \begin{cases} \text{deg}(i) & \text{if } i = j \\ 0 & \text{otherwise} \end{cases}$$

Note that  $\text{deg}(i) = \sum_{(i,j) \in S} \delta_{i,j} = \sum_j \delta_{i,j}$  With:  $\delta_{i,j} = 1$  if  $i$  is connected to  $j$ , 0 otherwise. Finally, the Laplacian matrix is defined as

$$L = D - A$$

The Laplacian matrix has a few interesting properties. It is positive semi-definite, and symmetric for an undirected graph.

Let's now assume we perform a cut in  $G$  (represented by a vector  $x$ ) to have two distinct graphs  $G_1 \subset G$ ,  $G_2 \subset G$ ,  $G_1 \cap G_2 = \emptyset$ . The cut vector is defined as

$$x_i = \begin{cases} 1 & \text{if } i \in G_1 \\ -1 & \text{if } i \in G_2 \end{cases}$$

The quadratic form of  $x^T L x$  gives

$$x^T L x = \sum_i \sum_j \delta_{i,j} x_i^2 - \sum_i \sum_j w_{i,j} x_i x_j \quad (9)$$

At this stage, note that

$$\begin{aligned} x_i^2 &= 1 \\ x_i = x_j &\Rightarrow x_i x_j = 1 \quad (i, j) \text{ is an uncut edge} \\ x_i = -x_j &\Rightarrow x_i x_j = -1 \quad (i, j) \text{ is a cut edge} \end{aligned}$$

We can rewrite (9) as

$$x^T Lx = \underbrace{\sum_i \sum_j \delta_{i,j}}_{\text{number of edges in } G} - \sum_{(i,j)\text{uncut}} w_{i,j} + \sum_{(i,j)\text{cut}} w_{i,j} \quad (10)$$

Hence maximizing (10) is equivalent to finding a cut that splits  $G$  into the two most-distant parts. Due to the Laplacian matrix properties, this is equivalent to finding the highest eigenvalue and using the corresponding eigenvector to perform the cut (detailed derivations are given in [34]). The spectral graph partitioning algorithm can be written as

---

**Algorithm 1:** Spectral graph partition (SGP)

---

**input** :  $G$  a weighted graph

**output:**  $G' = G_1 \cup G_2$  with  $G_1 \subset G, G_2 \subset G$  distinct graphs,  
 $G_1 \cap G_2 = \emptyset$

$L$ : Laplacian of  $G$ ;

$v, \lambda$  eigenvectors and associated values of  $L$ ;

Get the maximum eigenvalue and associated vector:

$$v^{\max}, \lambda^{\max} = \max_{\lambda} \lambda ;$$

$$m = \text{median}(v^{\max});$$

Construct cut vector  $x$  as:  $x_i = \begin{cases} 1 & \text{if } v_i^{\max} \geq m ; \\ -1 & \text{if } v_i^{\max} < m \end{cases}$ ;

$$G_1, G_2 = \text{cut}(G, x);$$

$$G' = G_1 \cup G_2 ;$$

**return**  $G'$

---

A graphical example of a single cut through a graph using the graph partitioning algorithm is pictured in fig. 5.

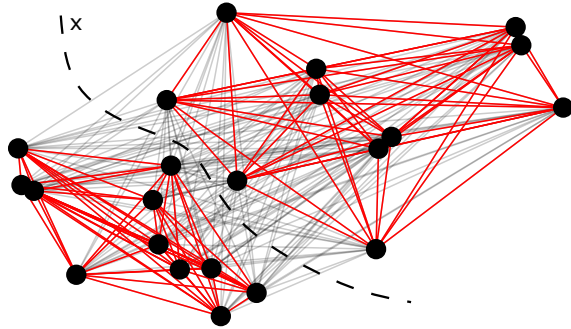


Figure 5: Illustration of a single cut in a random graph, represented by its nodes (black dots) and edges (gray and red lines)

This approach can be used to successively cut the original graph into smaller partitions until the size of a sub-graph is smaller than  $2k$  for  $k$  the desired graph size. The resulting clusters will have a size between  $k$  and  $2k - 1$  as illustrated in fig. 6. For  $k > 2$ , this can lead to significant unbalance. An IP formulation could be used to further reduce the imbalance when the next graph to cut has a relatively small number of nodes.

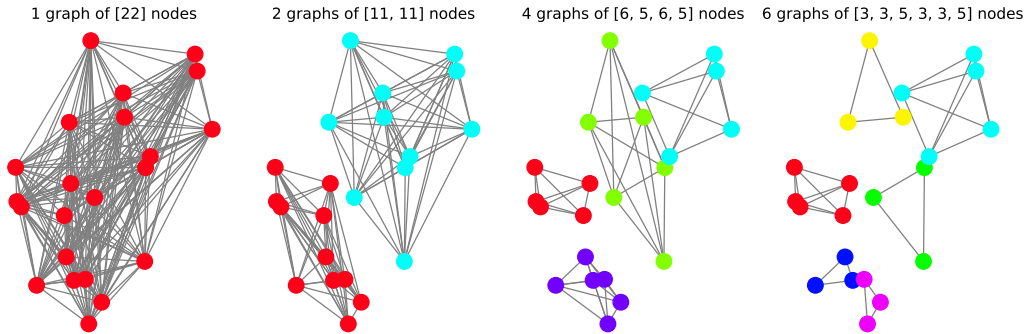


Figure 6: Illustration of successive (from left to right) spectral graph partitioning

### 2.2.3. Recursive spectral graph partitioning

The spectral graph partitioning has low complexity and ensures more or less balanced clusters when applied successively. In contrast, the IP formulation of the graph partitioning problem provides the most optimal balancing of the graph partitioning, but the computational complexity makes it unusable for large graphs. To gain the best of the two worlds, we propose the

following recursive spectral graph partitioning (RSGP) algorithm:

---

**Algorithm 2:** Recursive spectral graph partition (RSGP)

---

**input** :  $G$  a weighted graph,  $k$  the desired partition size

**output:**  $G' = \bigcup_{j=1}^J G_j$  with  $G_j$  a set of distinct graphs  
 $G_j \subset G, G_l \cap G_k = \emptyset \quad l, k = [1 \dots J] \quad l \neq k$

$[G_1, G_2] = \text{SGP}(G)$ : cut of  $G$  using spectral graph partitioning  
(algorithm 1) ;

$G'$ : an empty graph ;

**for**  $i$  in  $[1, 2]$  **do**

$N_i$  : number of nodes in  $G_i$ ;

**if**  $3k \leq N_i < 4k$  **then**

$G'_i$ : apply IP formulation to partition  $G_i$  (8) ;

**else if**  $N_i \geq 2k$  **then**

$G'_i = \text{RSGP}(G_i)$ ;

**else**

$G'_i = G_i$ ;

**end**

$G' = G' \cup G'_i$ ;

**end**

**return**  $G'$

---

The comparison of the partitioning of the graph with 22 nodes into clusters of three records using SGP, RSGP, and IP is presented in fig. 7. In terms of unbalance ( $\sum_g N_g - k$ , with  $N_g$  the  $g^{\text{th}}$  partition size), the proposed RSGP algorithm lies in between the successive SGP algorithm and the IP optimization (RSGP's unbalance is four vs. six for SGP, and one for IP). However, the RSGP computing time does not increase exponentially with the number of nodes, as shown in fig. 8.

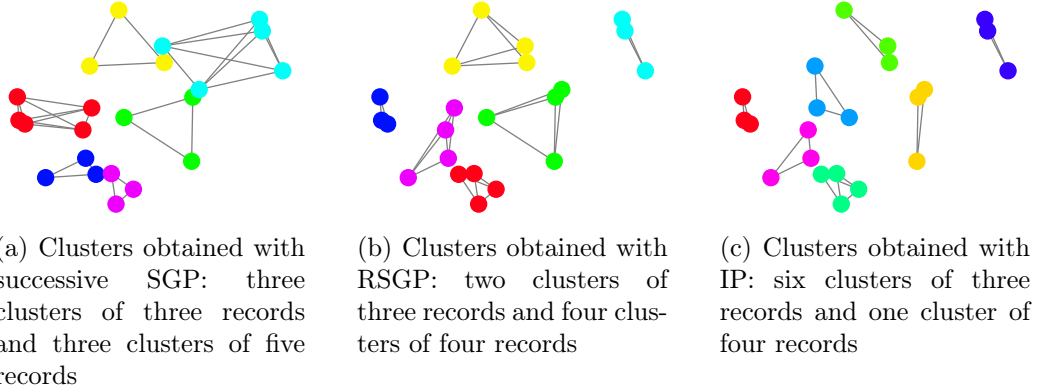


Figure 7: Comparison of the partitioning of 22 nodes with the SGP, RSGP, and IP methods

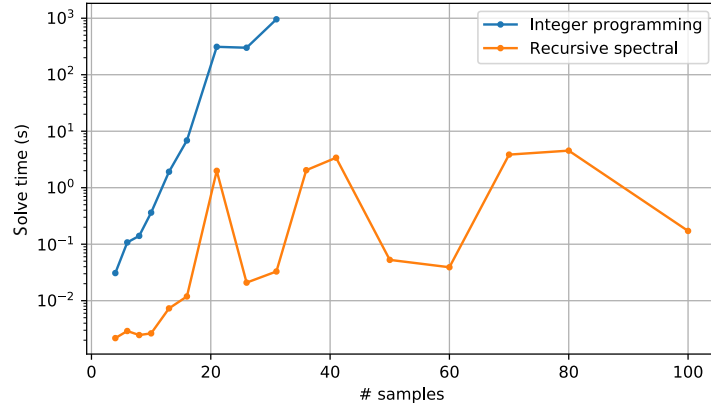


Figure 8: Computation time comparison

Hence, the RSGP algorithm is suitable for partitioning large datasets into small groups of equal size and fulfilling the requirements for grouping SM measurements for anonymisation purposes. So far, the definition of the SM features (the record attributes) has not been discussed. Indeed the feature selection depends on the ultimate goal of the study, as it will determine which load characteristics are significant and how similarity is defined. Provided that the selected SM features (i.e. load characteristics) best reflect the goal of the analysis, the RSGP supposes that any intra-group permutation of one SM by another will provide similar results. In this work, we assume that the

SM data are used for "network simulations". For this specific end use, we will discuss the most appropriate features.

### 3. Benchmark

We have proposed two methods to enable network simulations using real load measurements:

- The load profiles allocation technique
- the load profiles anonymisation technique

To validate these two approaches and compare their performance with respect to network simulations, we solve the load-flow equation using reference loads. The load-flow problem allows us to calculate the buses' voltage ( $V_{b,t}$   $b \in$  Bus set), lines' current ( $I_{l,t}$   $l \in$  line set), and the power at the substation (transformer power  $P_i^{\text{trafo}}$ ) at all time  $t \in T$ . The load-flow is then solved using the loads resulting either from the load allocation technique or from one random permutation resulting from the anonymisation technique. The performance of the two methods are measured using dedicated key performance indicators:

$$\text{Voltage magnitude mean squared error} \quad \text{MSE}_{\text{vm}} = \sum_{t=1}^T \sum_{b=1}^B \frac{(V_b - V_b^{\text{ref}})^2}{B} \quad (11)$$

$$\text{Maximum transformer loading error} \quad \text{E}_{\text{maxTRL}} = \frac{P_{\text{max}}^{\text{trafo}} - P_{\text{max}}^{\text{trafo,ref}}}{P_{\text{max}}^{\text{trafo,ref}}} \quad (12)$$

$$\text{Maximum line loading error} \quad \text{E}_{\text{maxLNL}} = \frac{I_{\text{max}} - I_{\text{max}}^{\text{ref}}}{I_{l,t}^{\text{ref}}} \quad (13)$$

$$\text{Minimum voltage error} \quad \text{E}_{\text{minVM}} = \frac{V_{\text{max}} - V_{\text{min}}^{\text{ref}}}{V_{\text{min}}^{\text{ref}}} \quad (14)$$

where subscripts min and max denote the minimum or maximum over the time and element index ( $b$  for the buses,  $l$  for the lines,  $i$  for the transformers), superscript ref indicates the reference case values.

### 3.1. Reference case

The DSO *Romande Energie* deployed SMs in the Rolle area. Those data are not accessible for privacy reasons, as explained above. In this work, we assume that if at least three customers are metered by SMs for a given location in a network, aggregating the consumption to a single virtual SM is enough to preserve individual customers' privacy. This is typically the case for multi-family buildings. In this case, the original SM measurements have been aggregated and only the resulting consumption has been provided. Those SMs are attributed to their actual network location. If two or more meters measure the same customer's consumption (measuring different circuits), they are also considered as one single SM and aggregated together (their location in the network is not known). All other SM measurements have been allocated in the networks by matching their annual energy consumption with the estimated building consumption (using the SIA norms [40] and a method inspired by [41]). The matching basically consists of minimizing the sum of the difference between the buildings' and SMs' annual energy consumption.

Finally, SMs that appear to measure consumption and production (a PV system in a self-consumption scheme) have been discarded. In the end, 257 SM measurements are used in this reference case. The annual energy consumption and network lines from six low-voltage networks are shown in fig. 9.

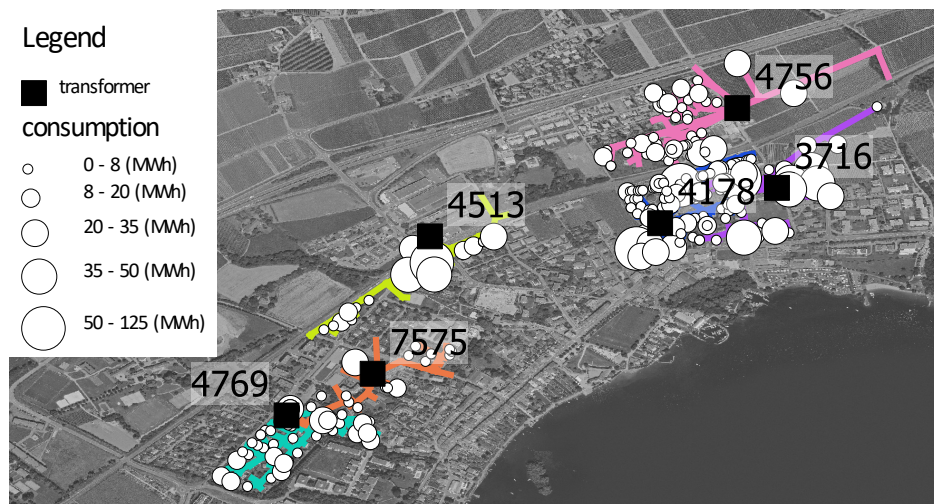


Figure 9: Map of the six networks' and reference loads' annual consumption. The numbers next to the transformers indicate the network ID.

### 3.2. Load allocation database and parameters

For the load allocation method, a database of SM measurements is required. The loads are split into three categories: Apartment, House, and Not residential (hereafter Not res.). The load database gathers SM measurements from a large set of (non-)residential sites. The measurements were acquired during the FLEXI [42], and FLEXI 2 [43] projects. These projects concerned networks outside the Rolle area. The number of loads in the database (reported in table 4) has to be compared with the number of loads present in each network and category (table 3). The parameter  $k^h$ , representing the maximum number of allocations of a load in a particular network, is obtained by dividing the number of loads in the network by the number of loads in the database for a given category. All measurements have a resolution of 15 mins and cover one year. The energy and power tolerances for the allocation ( $\epsilon_E$  and  $\epsilon_P$ ) are set to 5 and 1%, respectively.

Table 3: Number of loads per category ("Not res." means not residential) and median annual consumption for each network (TR#)

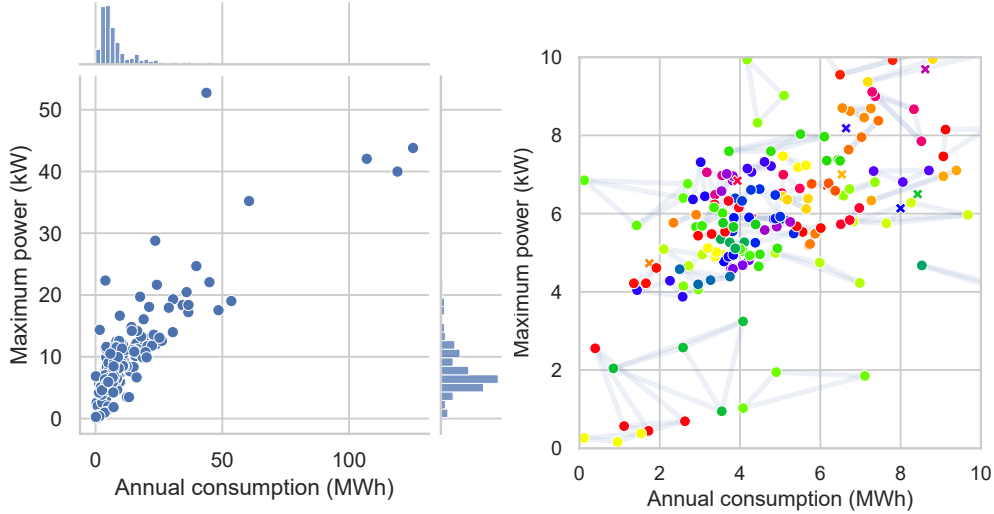
TR #	Category	# load	Median cons. (MWh)
3716	Apartment	13	11.2
	House	15	5.4
	Not res.	22	11.6
4178	Apartment	9	20.2
	House	51	4.5
	Not res.	6	10.0
4513	Apartment	18	4.1
	House	3	3.7
	Not res.	9	11.0
4756	Apartment	3	4.3
	House	28	5.4
	Not res.	18	9.9
4769	Apartment	4	4.2
	House	26	4.9
	Not res.	14	12.5
7575	Apartment	2	65.9
	House	11	4.9
	Not res.	5	5.1

Table 4: Number of loads per category (Not res. means not residential) and median annual consumption for each database source

Src.	Category	# load	Median cons. (MWh)
FLEXI	Apartment	38	3.3
	House	46	4.4
	Not res.	1	22.4
FLEXI 2	Apartment	44	2.1
	House	48	4.2
	Not res.		
<b>Not res.</b>		3	407

### 3.3. Smart-meter anonymisation method

As stated in the reference case description, *Romande Energy* provided the 257 SM measurements located in the six sub-networks. To mimic a real case, the measurements' true locations are unknown except for the measurements grouping three or more customers (39 loads in total). For all other loads, the SM anonymisation (SMANET) technique should be applied. The first step is to define the features of the loads. In a primary approach, the energy ( $E_i = \sum_t P_{i,t} \cdot TS_t$ ), and maximum power ( $P_i^{\max} = \max_t P_{i,t}$ ) are used as input features for the partitioning. (The features are plotted in fig. 10a.) The second step is to perform the partitioning using the RSGP method. For this step, the features are normalized to have zero mean and unity variance before the distance matrix  $D$  is calculated. The target group size is set to three loads. The resulting groups are shown in fig. 10b.



(a) Energy and maximum power distribution (b) Resulting groups colored by group ID

Figure 10: SM measurements' selected features and results of the partitioning

### 3.4. Features choice for SMANET

In a second approach, we measure the impact of the feature choice on the load-flow solution's accuracy. To do so, we define five partitioning scenarios:

**Energy and maximum power** These are the same features as defined in section 3.3, hereafter shortened "E + max P".

**Energy** Only the annual energy consumption is considered.

**PCA** From a set of features proposed by [44], we perform a principal component analysis (PCA) and keep the first  $N$  components that explain 99% of the dataset variance.

**Affinity** Again, E + max P are used as input features, but with the affinity matrix ( $A_{i,j} = 1/D_{i,j}$ ) instead of the distance matrix. In the RSGP, this would be equivalent to finding the partitioning with the largest intra-cluster variance.

**One group** Instead of grouping the loads by three, all (except those measuring more than three customers) are put into a single group.

The resulting four additional partitioning scenarios are illustrated in fig. 11. In these figures, we kept the projection on the energy - max Power plane. This can lead to unnatural cluster representations as for the PCA scenarios (fig. 11b). Note that for the Energy scenarios (fig. 11a), the clusters are formed by vertical slicing of the dataset.

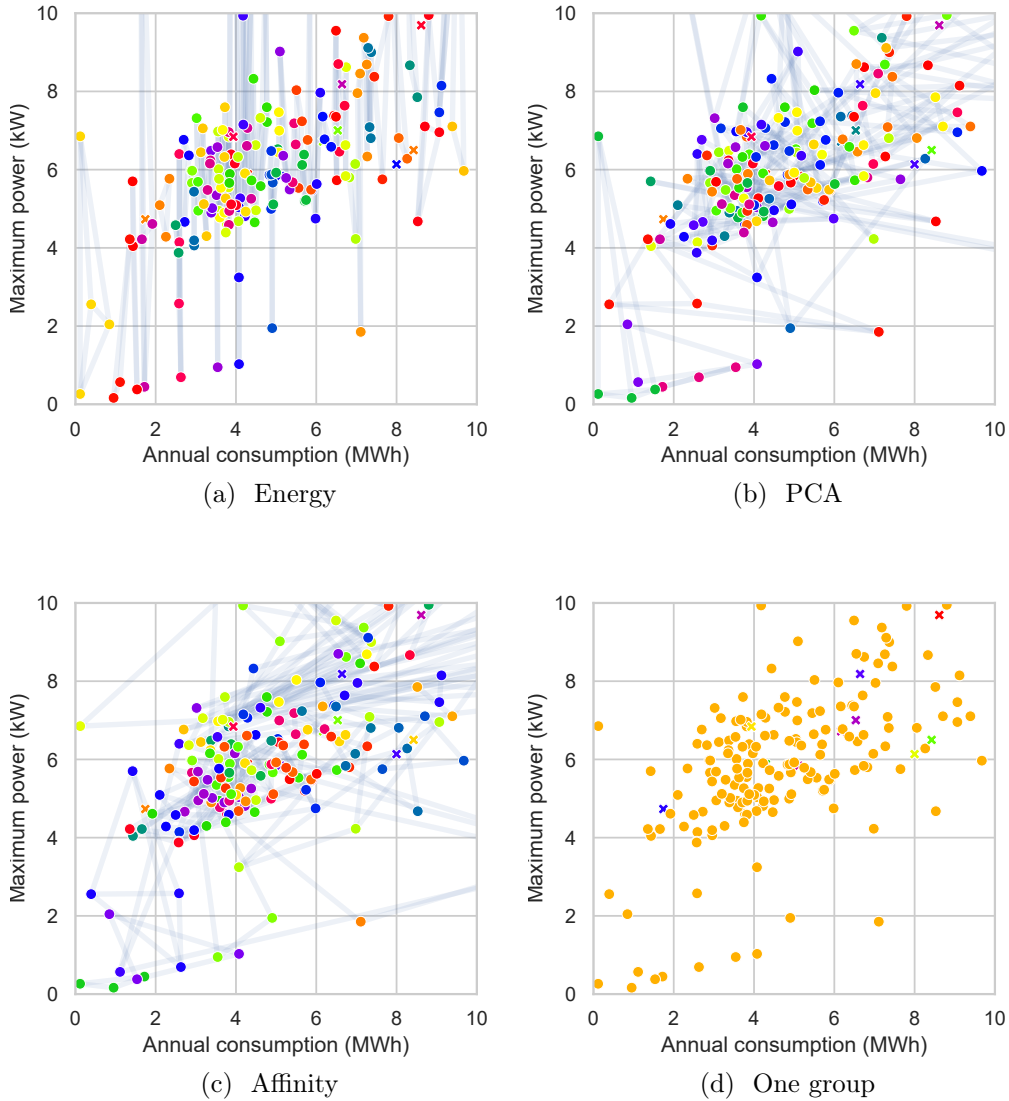


Figure 11: Four additional partitioning scenarios. Measurements with more than three customers are marked with a  $\times$ .

As described in the workflow of the SMANET methodology in fig. 3, the final stage is to randomly select one permutation of the buses per group and allocate each load to its bus. In this stage, to account for the stochastic nature of this method, the load-flow problem is solved 200 times, each time

with a new a new permutation of the bus-load assignment.

## 4. Results

### 4.1. Load allocation and SMANET comparison

The voltage error distribution across all times and all buses in the six networks are pictured in fig. 12. Here, only a single random permutation is used for the SMANET method. (The allocation provides by definition only one solution.) Both the allocation and the SMANET method give errors mostly below 0.002 pu, which are already sufficient for most network studies. The SMANET process seems to provide slightly smaller errors. These minor errors can be explained by the fact that during a large portion of the year, the active power demand is small compared to the network capacity (during the night, for instance), leading to a local voltage close to 1 pu.

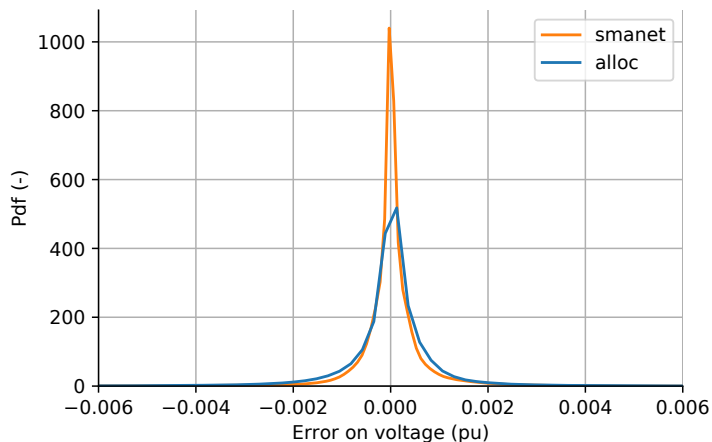


Figure 12: Voltage error distribution

To balance this effect, one must look at what is happening at the transformer nodes. The transformer's active power is plotted for the six networks for a particular day in fig. 13. This figure shows how the second-stage optimization of the allocation method improves transformer state estimation accuracy compared with the first-stage obtained power (blue dots). By definition, the maximum power deviation at the transformer should be smaller than 1%. For this reason, the allocated (stage 2) curve is very close to the true one. The resulting power at the transformer obtained with the SMANET

method also leads to very good results. The quality of this method also lies in the fraction of the network loads given by the measure of more than the required three customers. In other words, for a network where all loads are multi-family buildings with more than three apartments, all loads' locations are known, and the network state estimation is very accurate (and there is no need for the anonymisation methodology).

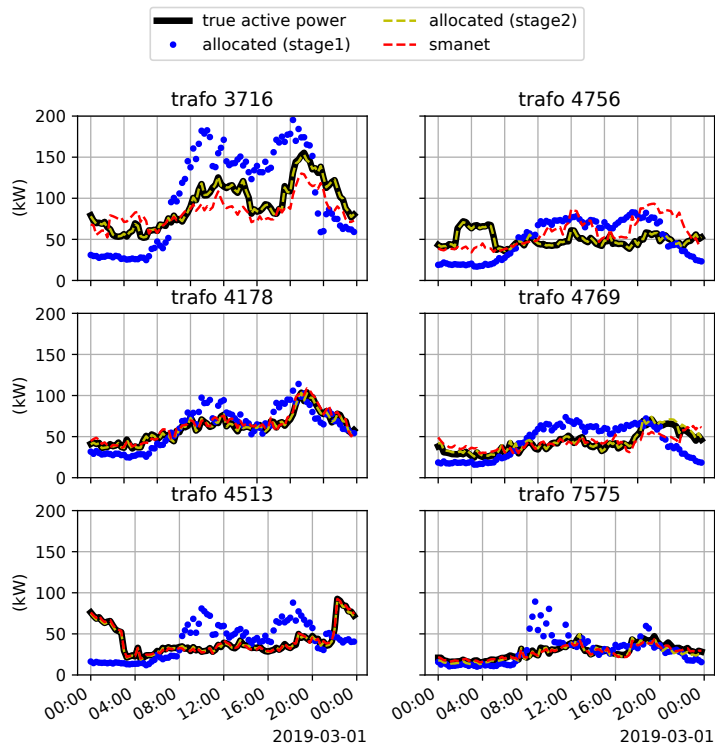
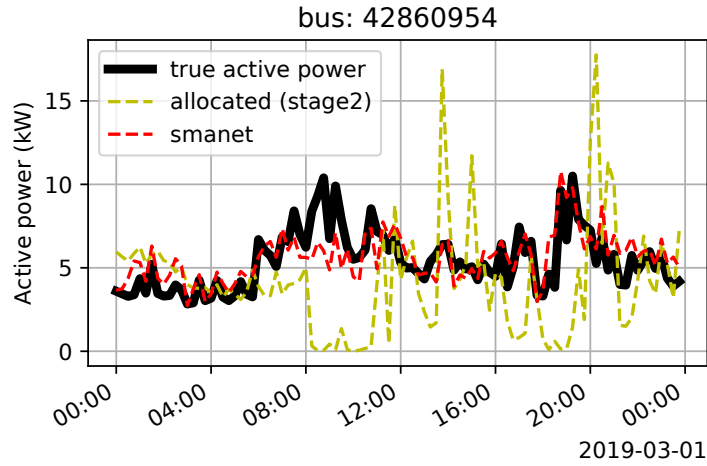
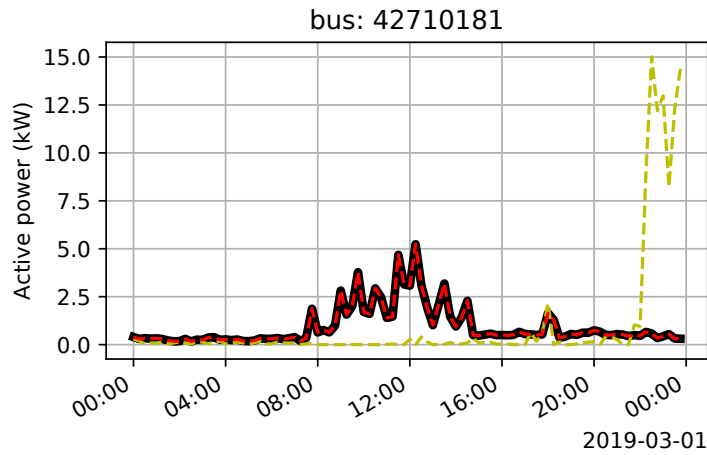


Figure 13: Active power at the transformer nodes of the six low-voltage grids

Despite the good voltage accuracy for both methods, the local power allocated to a given network location (bus) is closer to the true one with the SMANET method than with the allocation method (fig. 14). The illustrative example of fig. 14b shows that the SMANET benefits from the network location knowledge in some cases. It also happens that by chance (1 out of 3), the load allocated to this bus is the actual original load of this bus.



(a) Fully allocated load



(b) Naturally anonymised load

Figure 14: Example of active power at two buses

Finally, the key performance indicators are reported in table 5. Again thanks to prior knowledge of the load locations, the SMANET method is slightly more accurate. The minimum voltage estimation error is below 3% for both methods. The maximum transformer loading is underestimated by 19% for the SMANET methods versus 1.2% for the allocation methods. The advantage of the allocation method on this metric is the constraints on the transformer’s power that should be below 1% in this case. The additional

0.2% comes from the fact that no prior knowledge of the grid losses is used in the allocation (the transformer’s power is assumed to be the sum of the network loads, neglecting the line losses). The accuracy of the SMANET methods also depends on the loads’ final allocation, i.e. for a given bus, out of the three loads belonging to the corresponding group, which load is attributed to the bus. In addition, the loads’ intra-group similarity is critical to have accurate network state estimation. In the following, the latter is discussed by evaluating the five partitioning scenarios and running, for each scenario, the load-flow simulation 200 times.

Table 5: Performance indicators per network for the allocation (A) and SMANET (S) methods

		<b>Network ID:</b>	<b>3716</b>	<b>4178</b>	<b>4513</b>	<b>4756</b>	<b>4769</b>	<b>7575</b>
MSE <sub>vm</sub> ( $\cdot 10^{-7}$ pu <sup>2</sup> )	A		16.7	1.3	24.7	2.7	2.3	1.6
	S		6.8	0.5	0.6	8.0	2.0	0.3
E <sub>maxTRL</sub> (%)	A		1.2	-0.9	-0.5	-0.2	0.1	0.0
	S		-18.9	10.4	1.1	32.3	6.8	2.9
E <sub>maxLNL</sub> (%)	A		192.0	304.2	52.9	207.6	212.4	91.6
	S		2.4	0.0	0.0	-3.0	15.6	8.4
E <sub>minVM</sub> ( $\cdot 10^{-3}$ pu)	A		-27.0	-13.9	-5.6	-13.7	-4.9	-3.6
	S		1.6	-0.7	-0.6	-0.9	-4.2	-0.1

#### 4.2. Features’ influence on SMANET accuracy

As mentioned, to have a clear overview of the SMANET accuracy, the load flows are solved several times with a new load-bus assignment. The key performance indicators are recorded for each iteration. The voltage magnitude mean squared error (calculated for all buses at all times for all iterations until the  $i^{th}$  iteration) is plotted in fig. 15. This figure shows the convergence of the mean squared error for all partitioning scenarios.

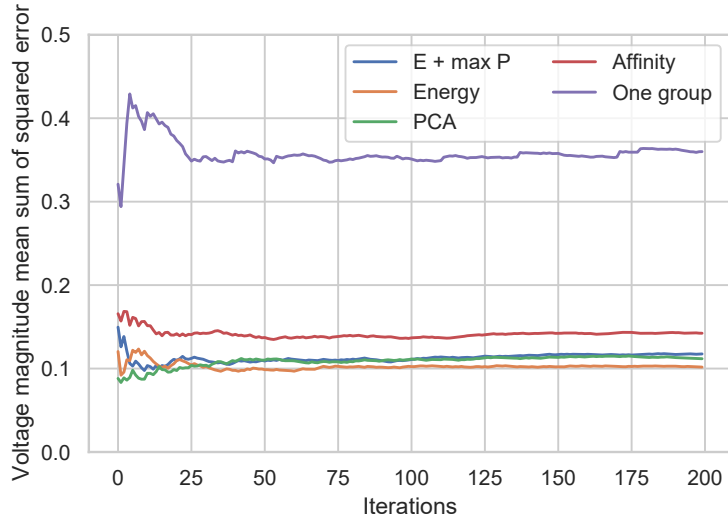


Figure 15: Voltage magnitude mean squared error convergence

The voltage magnitude error (across all times, buses, and iterations) is plotted in fig. 16. Again the error is mostly smaller than 0.002 pu. Except for the Dummy and One group scenarios, the three other scenarios provide similar accuracy from this perspective.

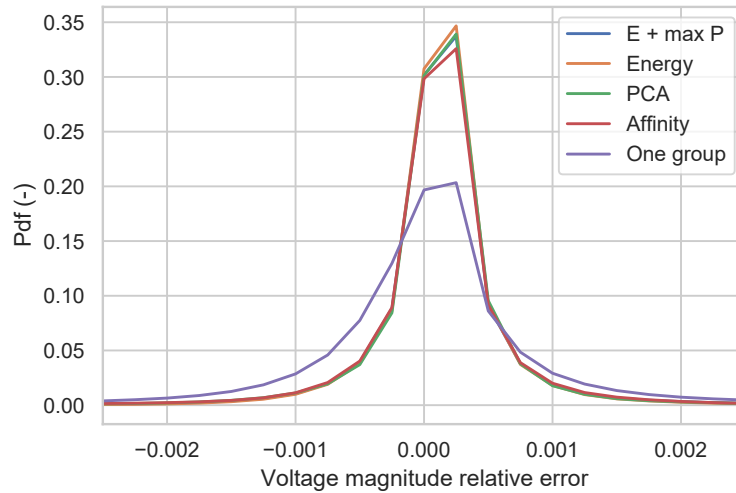


Figure 16: Error on voltage magnitude

The mean squared error of the voltage magnitude and its standard deviation (across iterations) are reported in table 6. Again no significant differences are observed between scenarios, except for the Affinity and One group scenarios that give slightly larger mean squared errors of the voltage magnitude.

Table 6: Mean squared error of the voltage magnitude for the five partitioning scenarios

	<b>E + max P</b>	<b>Energy</b>	<b>PCA</b>	<b>Affinity</b>	<b>One group</b>
<b>Mean</b>	$2.02 \cdot 10^{-8}$	$1.70 \cdot 10^{-8}$	$2.02 \cdot 10^{-8}$	$2.24 \cdot 10^{-8}$	$3.92 \cdot 10^{-8}$
<b>Std</b>	$7.66 \cdot 10^{-9}$	$6.84 \cdot 10^{-9}$	$9.05 \cdot 10^{-9}$	$7.18 \cdot 10^{-9}$	$1.68 \cdot 10^{-8}$

## 5. Discussion

The results highlight that both methods provide similar results in terms of network state estimation accuracy. In more detail, the SMANET approach provides slightly higher accuracy with respect to voltage estimation, which translates into higher accuracy in terms of line loading. The assumption that a load can be exchanged by an electrically similar load while still keeping accurate network simulations seems valid in this case. The allocation method provides better results in terms of transformer loading. The reason behind this observation is the applied constraints on the estimated active power at the transformer side. This linear constraint does not account for line losses nor for line inductance, which requires the provision of reactive power. Still, the results show that this does not have a significant impact. The SMANET approach suffers from a significant error in transformer loading. This is in contrast with its low estimation error on voltage and line loading. The SMANET approach should be preferred as soon as SM data are available inside a given network. When this is not the case, the allocation of SM measurements from an external network is the only suitable solution. The allocation and SMANET approaches could be combined. For the network locations where SMs are installed, the SMANET approach could be used. For the network locations where no SMs are currently set up, SM data acquired outside the considered networks could be allocated to these locations. In such a case, it would be better to use load profiles from another network than to just reuse the one measured in the same network to avoid simultaneous peaks. However, if not possible, the second-stage optimization of the allocation method should reduce this issue by deforming the loads.

Both approaches rely on the fact that SMs are considered anonymous if the true location of the original meter is not known. However, the allocation approach relies on labeling to define load categories. The numbers of these categories could be extended, but it might raise issues if the label gets so precise that it allows the true origin of the meter to be linked with the SM measurements. These categories could be based on publicly available data regarding buildings, e.g. from the cantonal/federal building registries. The registries contain more information on the buildings that could improve the classification of the loads, thus the accuracy of the network simulation. The degree of anonymisation in the SMANET approach becomes questionable when groups with a large intra-distance occur, i.e. if a group contains three very significantly different annual energy consumption values. In this case, given the fact that three possible locations for these loads are provided, it might be easy to deduce the true location of the loads, as pointed out by [33]. This can be addressed first by increasing the dataset size, second by increasing the group size, and finally by excluding those loads from the dataset. Besides, in this work, we consider only six low-voltage networks and the corresponding installed SMs. The extension of the SMANET methodology to an entire DSO control area raises the following question: Should all SM data be encompassed in a single dataset, or is it possible to split the dataset by geographical area? In this work, we consider only one sufficiently large dataset and discussed the limitation of such methodologies. It might be worth combining the knowledge gained from information theory to tackle this question.

## 6. Conclusion

In this work, two methods to use SMs for network simulations were proposed. The first method was based on an allocation approach. First, the allocation was formulated as a mixed-integer problem to allocate loads from a database to the network locations based on the annual energy demand difference. Second, an adjustment stage deformed the original loads to match the power at the transformer.

The second method aimed to anonymise the smart measurements extracted from a given set of networks by grouping the SM loads by  $K$  and linking this group to a set of  $K$  network locations (buses). The final load-bus allocation was achieved by randomly assigning a load to a bus in the considered group. This method allowed for stochastic analysis of the network stage (by randomly permuting the assignment). A stochastic approach improved

the quality of the network simulation but at a higher computational burden. This approach showed the best accuracy with respect to state estimation and voltage magnitude estimation. Line loading errors were significant as they result from an accumulation of downstream load errors.

Both methods allow for an anonymised usage of SM data for network simulations. Thus they are particularly useful for DSOs. Combining both methods could prove useful. As the rollout of SMs is just starting, some networks might contain very few or no SMs at all. A combination of both approaches could allow for a smooth transition from a low SM density to a future with all customers equipped with SMs.

## 7. Acknowledgement

This work was supported by InnoSuisse in the framework of the SCCER-FURIES. We would like to thank the team from *Romande Energie*, Patrizio Canzi, Kim Leng Chhun, Assia Garbinato, Tiago Torrado, and Arnaud Bifrare for their help and precious support.

## References

- [1] F. D. Garcia, F. P. Marafao, W. A. D. Souza, L. C. P. D. Silva, Power Metering: History and Future Trends, IEEE Green Technologies Conference (2017) 26–33doi:10.1109/GreenTech.2017.10.
- [2] Y. Wang, Q. Chen, T. Hong, C. Kang, Review of Smart Meter Data Analytics: Applications, Methodologies, and Challenges, IEEE Transactions on Smart Grid (2018) 1–1arXiv:1802.04117, doi:10.1109/TSG.2018.2818167.  
URL <https://arxiv.org/pdf/1802.04117.pdf><http://arxiv.org/abs/1802.04117><http://dx.doi.org/10.1109/TSG.2018.2818167><http://ieeexplore.ieee.org/document/8322199/>
- [3] J. Zheng, D. W. Gao, L. Lin, Smart meters in smart grid: An overview, IEEE Green Technologies Conference (2013) 57–64doi:10.1109/GreenTech.2013.17.
- [4] G. Hart, Nonintrusive appliance load monitoring, Proceedings of the IEEE 80 (12) (1992) 1870–1891. doi:10.1109/5.192069.  
URL <http://ieeexplore.ieee.org/document/192069/>

- [5] A. Zoha, A. Gluhak, M. Imran, S. Rajasegarar, Non-Intrusive Load Monitoring Approaches for Disaggregated Energy Sensing: A Survey, *Sensors* 12 (12) (2012) 16838–16866. doi:10.3390/s121216838.  
URL <http://www.mdpi.com/1424-8220/12/12/16838/http://www.mdpi.com/1424-8220/12/12/16838>
- [6] J. Holweger, M. Dorokhova, L. Bloch, C. Ballif, N. Wyrsh, Un-supervised algorithm for disaggregating low-sampling-rate electricity consumption of households, *Sustainable Energy, Grids and Networks* 19 (2019) 100244. arXiv:1908.10713, doi:10.1016/j.segan.2019.100244.  
URL <https://doi.org/10.1016/j.segan.2019.100244>
- [7] B. Zhao, M. Ye, L. Stankovic, V. Stankovic, Non-intrusive load disaggregation solutions for very low-rate smart meter data, *Applied Energy* 268 (2020) 114949. doi:10.1016/j.apenergy.2020.114949.  
URL <https://linkinghub.elsevier.com/retrieve/pii/S030626192030461X>
- [8] Z. A. Khan, D. Jayaweera, M. S. Alvarez-Alvarado, A novel approach for load profiling in smart power grids using smart meter data, *Electric Power Systems Research* 165 (January) (2018) 191–198. doi:10.1016/j.epsr.2018.09.013.  
URL <https://doi.org/10.1016/j.epsr.2018.09.013>
- [9] F. Pilo, G. Pisano, S. Ruggeri, M. Troncia, Data analytics for profiling low-voltage customers with smart meter readings, *Applied Sciences (Switzerland)* 11 (2) (2021) 1–30. doi:10.3390/app11020500.
- [10] J. Ponocko, J. V. Milanovic, Forecasting Demand Flexibility of Aggregated Residential Load Using Smart Meter Data, *IEEE Transactions on Power Systems* 33 (5) (2018) 5446–5455. doi:10.1109/TPWRS.2018.2799903.
- [11] Z. A. Khan, D. Jayaweera, Approach for smart meter load profiling in Monte Carlo simulation applications, *IET Generation, Transmission and Distribution* 11 (7) (2017) 1856–1864. doi:10.1049/iet-gtd.2016.2084.

- [12] M. Z. Degefa, R. J. Millar, M. Koivisto, M. Humayun, M. Lehtonen, Load Flow Analysis Framework for Active Distribution Networks Based on Smart Meter Reading System, *Engineering* 05 (10) (2013) 1–8. doi:10.4236/eng.2013.510a001.
- [13] A. Bahmanyar, A. Estebarsari, A. Bahmanyar, E. Bompard, Nonsy load flow: Smart grid load flow using non-synchronized measurements, in: 2017 IEEE International Conference on Environment and Electrical Engineering and 2017 IEEE Industrial and Commercial Power Systems Europe (EEEIC / I&CPS Europe), IEEE, 2017. doi:10.1109/eeeic.2017.7977509.
- [14] S. Bhela, V. Kekatos, S. Veeramachaneni, Enhancing observability in distribution grids using smart meter data, *IEEE Transactions on Smart Grid* 9 (6) (2018) 5953–5961. arXiv:1612.06669, doi:10.1109/TSG.2017.2699939.
- [15] M. M. Othman, M. H. Ahmed, M. M. Salama, A novel smart meter technique for voltage and current estimation in active distribution networks, *International Journal of Electrical Power and Energy Systems* 104 (June 2018) (2019) 301–310. doi:10.1016/j.ijepes.2018.07.015. URL <https://doi.org/10.1016/j.ijepes.2018.07.015>
- [16] A. Cataliotti, V. Cosentino, D. Di Cara, P. Russotto, E. Telaretti, G. Tine, An Innovative Measurement Approach for Load Flow Analysis in MV Smart Grids, *IEEE Transactions on Smart Grid* 7 (2) (2016) 889–896. doi:10.1109/TSG.2015.2430891.
- [17] F. Ni, P. H. Nguyen, J. F. Cobben, H. E. Van den Brom, D. Zhao, Three-phase state estimation in the medium-voltage network with aggregated smart meter data, *International Journal of Electrical Power and Energy Systems* 98 (February 2017) (2018) 463–473. doi:10.1016/j.ijepes.2017.12.033.
- [18] S. Wan Yen, S. Morris, M. A. Ezra, T. Jun Huat, Effect of smart meter data collection frequency in an early detection of shorter-duration voltage anomalies in smart grids, *International Journal of Electrical Power and Energy Systems* 109 (January) (2019) 1–8. doi:10.1016/j.ijepes.2019.01.039. URL <https://doi.org/10.1016/j.ijepes.2019.01.039>

- [19] D. Chen, S. Barker, A. Subbaswamy, D. Irwin, P. Shenoy, Non-intrusive occupancy monitoring using smart meters, in: Proceedings of the 5th ACM Workshop on Embedded Systems For Energy-Efficient Buildings, ACM, 2013, pp. 1–8. doi:10.1145/2528282.2528294.
- [20] V. Becker, W. Kleiminger, Exploring zero-training algorithms for occupancy detection based on smart meter measurements, Computer Science - Research and Development 33 (1-2) (2017) 25–36. doi:10.1007/s00450-017-0344-9.
- [21] R. Razavi, A. Gharipour, M. Fleury, I. J. Akpan, Occupancy detection of residential buildings using smart meter data: A large-scale study, Energy and Buildings 183 (2019) 195–208. doi:10.1016/j.enbuild.2018.11.025.
- [22] A. Allik, S. Muiste, H. Pihlap, Smart meter data analytics for occupancy detection of buildings with renewable energy generation, in: 2020 9th International Conference on Renewable Energy Research and Application (ICRERA), IEEE, 2020. doi:10.1109/icrera49962.2020.9242830.
- [23] M. Dorokhova, F. Ribeiro, A. Barbosa, J. Viana, F. Soares, N. Wyrsh, Real-world implementation of an ICT-based platform to promote energy efficiency, Energies 14 (9) (2021) 2416. doi:10.3390/en14092416.
- [24] S. Zhou, M. A. Brown, Smart meter deployment in Europe: A comparative case study on the impacts of national policy schemes, Journal of Cleaner Production 144 (2017) (2017) 22–32. doi:10.1016/j.jclepro.2016.12.031.  
URL <http://dx.doi.org/10.1016/j.jclepro.2016.12.031>
- [25] L. Sankar, S. Raj Rajagopalan, S. Mohajer, H. Vincent Poor, Smart meter privacy: A theoretical framework, IEEE Transactions on Smart Grid 4 (2) (2013) 837–846. doi:10.1109/TSG.2012.2211046.
- [26] S. R. Rajagopalan, L. Sankar, S. Mohajer, H. V. Poor, Smart meter privacy: A utility-privacy framework, 2011 IEEE International Conference on Smart Grid Communications, SmartGridComm 2011 (2011) 190–195arXiv:1108.2234, doi:10.1109/SmartGridComm.2011.6102315.
- [27] E. McKenna, I. Richardson, M. Thomson, Smart meter data: Balancing consumer privacy concerns with legitimate applications, Energy Policy

41 (2012) 807–814. doi:10.1016/j.enpol.2011.11.049.  
URL <http://dx.doi.org/10.1016/j.enpol.2011.11.049>

- [28] C. Efthymiou, G. Kalogridis, Smart Grid Privacy via Anonymization of Smart Metering Data, 2010 First IEEE International Conference on Smart Grid Communications (2010) 238–243doi:10.1109/smartgrid.2010.5622050.
- [29] T. Jakobi, S. Patil, D. Randall, G. Stevens, V. Wulf, It Is About What They Could Do with the Data, ACM Transactions on Computer-Human Interaction 26 (1) (2019) 1–44. doi:10.1145/3281444.
- [30] M. R. Asghar, G. Dán, D. Miorandi, I. Chlamtac, Smart meter data privacy: A survey, IEEE Communications Surveys and Tutorials 19 (4) (2017) 2820–2835. doi:10.1109/COMST.2017.2720195.
- [31] M. A. Mustafa, S. Cleemput, A. Aly, A. Abidin, A secure and privacy-preserving protocol for smart metering operational data collection, IEEE Transactions on Smart Grid 10 (6) (2019) 6481–6490. arXiv:1801.08353, doi:10.1109/TSG.2019.2906016.
- [32] M. Gough, S. Santos, T. Alskaf, M. Javadi, R. Castro, J. P. Catalao, Preserving Privacy of Smart Meter Data in a Smart Grid Environment, IEEE Transactions on Industrial Informatics 3203 (c) (2021) 1–10. doi:10.1109/TII.2021.3074915.
- [33] G. Eibl, S. Taheri-Boshrooyeh, A. Küpçü, Aggft: Low-cost fault-tolerant smart meter aggregation with proven termination and privacy (Feb. 2021). arXiv:2102.09429.
- [34] C. Schulz, Course Notes : Graph Partitioning and Graph Clustering in Theory and Practice, Karlsruhe Institute of Technology (KIT), Karlsruhe, 2015.
- [35] D. Chakraborty, S. Das, Modified fuzzy c-mean for custom-sized clusters, Sādhanā 44 (8) (jul 2019). doi:10.1007/s12046-019-1166-1.
- [36] P. Prosser, Stable roommates and constraint programming, in: Integration of AI and OR Techniques in Constraint Programming, Springer International Publishing, 2014, pp. 15–28. doi:10.1007/978-3-319-07046-9-2.

- [37] K. Iwama, S. Miyazaki, K. Okamoto, Stable roommates problem with triple rooms (01 2007).
- [38] J. D. Lichtman, On the Multidimensional Stable Marriage Problem (Sep. 2015). [arXiv:1509.02972](https://arxiv.org/abs/1509.02972).
- [39] A. Miyauchi, T. Sonobe, N. Sukegawa, Exact clustering via integer programming and maximum satisfiability, Proceedings of the AAAI Conference on Artificial Intelligence 32 (1) (Apr. 2018).  
URL <https://ojs.aaai.org/index.php/AAAI/article/view/11519>
- [40] SIA, Donnees d'utilisation des locaux pour l'energie et les installations du batiment, Tech. rep., Swiss society of engineers and architects, Zurich (2015).
- [41] L. Girardin, A GIS-based Methodology for the Evaluation of Integrated Energy Systems in Urban Area, École Polytechnique Fédérale de Lausanne Doctoral thesis 5287 (2012) 100–101. [doi:10.5075/epfl-thesis-5287](https://doi.org/10.5075/epfl-thesis-5287), [urn:nbn:ch:bel-epfl-thesis5287-5](https://nbn-resolving.org/urn:nbn:ch:bel-epfl-thesis5287-5).  
URL <https://infoscience.epfl.ch/record/170535>
- [42] L. Perret, J. Fahrni, N. Wyrsh, Y. Riesen, S. Puddu, S. Weber, D. Pfacheco Barzallo, FLEXI Determining the flexibilization potential of the electricity demand, Tech. rep., Federal Office For Energy (2015).
- [43] L. Perret, Y. Chevillat, N. Wyrsh, L. Bloch, J. Holweger, S. Weber, M. Péclat, Flexi 2 Déterminer le potentiel de flexibilisation de la demande d'électricité des ménages, Tech. rep., Fedral Office For Energy (2019).
- [44] C. Beckel, L. Sadamori, S. Santini, Towards automatic classification of private households using electricity consumption data, in: Proceedings of the Fourth ACM Workshop on Embedded Sensing Systems for Energy-Efficiency in Buildings - BuildSys '12, ACM, 2012, p. 169. [doi:10.1145/2422531.2422562](https://doi.org/10.1145/2422531.2422562).  
URL <http://dl.acm.org/citation.cfm?doid=2422531.2422562>